Advanced Materials and Technologies for Environmental Applications - AdvMatTechEnv
Open Acces Journal
powered by SciEdTech

Iron Removal from Ground Water using Egyptian Cost-Effective Clay Minerals

Hamdy Maamoun ABDEL-GHAFAR[1,*], Elsayed Ali ABDEL-AAL[1] and Bahgat Ezat EL ANADOULI[2]

[1] Central Metallurgical Research and Development Institute (CMRDI), P.O. Box: 87 Cairo, Egypt
(* hamdy.maamoun@yahoo.com);

[2] Cairo University, Faculty of Science, Cairo, Egypt

Article History

Received 2 February 2018
Revised 16 February 2018
Accepted 19 February 2018

Keywords:

Glauconite
Kaolin
Iron removal
Statistical design
Box-Behnken

Abstract:

Glauconite and kaolin was used as adsorbent materials for iron ion removal from synthetic solutions. Different concentrations of iron solution have been prepared 10, 20 and 30 mg/L. Different doses of glauconite and kaolin were added 0.1, 0.55 and 1.0 g. Statistical design was used to determine the optimum conditions of iron adsorption on glauconite and kaolin. It is shown that glauconite has high adsorption for iron reaching up to 95% while kaolin exhibit lower adsorption for iron. Physical and chemical characterization of glauconite and kaolin was done and these data were correlated with the removal efficiency. Higher surface area of glauconite 19.8 m^2/g compared to kaolin 5.4 m^2/g lead to higher removal efficiency.

1. Introduction

Glauconite and kaolin clays are extremely fine particles exhibiting chemical properties of colloids [1, 2]. The high specific surface area, chemical and mechanical stability, layered structure; high cation exchange capacity (CEC) made these clays excellent adsorbent materials [3]. Because of their small particle size, the specific surface area (external and internal) of clays and clay minerals could be increased to few hundreds m^2/g. Natural clays like glauconite and kaolin acquire prominence as low-cost adsorbents over the last few decades due to their abundance and its capability to undergo modification to enhance the surface area and adsorption capacity [4].

Ground water and some water from the bottom anoxic zones of reservoirs often contain iron and manganese ions or their complexes with natural organic matter [5, 6]. In conventional treatment, the oxidation of iron and manganese was carried out using various oxidants such as oxygen, chlorine, ozone, or potassium permanganate. The chemistry of oxidation becomes complicated when background species such as phosphate and fulvic acid are involved, so that the oxidation of ferrous ion, that can be normally readily oxidized, is retarded [7].

It was reported that, heavy metals such as arsenic, cadmium, copper, cobalt, chromium, nickel, iron, and zinc, exist in variable contents in drinking water as well as in ground water [8, 9]. This makes the removal of these toxic contaminants from water sources, efficiently and within reasonable costs, an important issue. Many adsorption materials have been investigated for the removal of heavy metal ions from water. Sorbents that have been studied include natural and artificial materials such as clay minerals [10-15], carbon-nanomaterials [16-19], biosorbents [20], and micro/nano-structured metal oxides [20-28].

In this research, adsorption of iron ions on glauconite and kaolin minerals was studied. In Egypt, ground water of New Valley area contains higher contents of iron ions above the acceptable limit. The concentrations of iron ions in New Valley ground waters are ranged from low to moderate. Baharia oasis area, Egypt is rich with glauconite, also Klabbsha, Aswan and Sinai areas, Egypt have a huge amount of kaolin. So, glauconite and kaolin can be used as a cost effective clay minerals for iron removal from ground water.

2. Experimental

2.1. Materials

Glauconite was obtained from New-Vally area, Egypt. Kaolin was obtained from Aswan area, Egypt. Samples were crushed, ground, sieved to -150+200 mesh size, and dried at 105°C. Samples of natural glauconite and kaolin analysis are given in Table 1. Physical properties of glauconite and kaolin were represented in Table 2.

A stock solution of ferrous ions (1000 mg/L Fe^{2+}) is prepared by dissolution of ferrous sulfate heptahydrate (Sigma-Aldrich chemicals, Germany) with distilled water. Then, different concentrations ferrous ions were prepared by dilution certain volume of stock solution with distilled water. All chemicals used were of analytical grade.

2.2. Methods

Experimental Statistical Design-Expert 9.0.3, Stat-Ease, Inc., MN, USA, software was used in this paper: 17 runs were carried out by applying the experimental Box-Behnken statistical design with three levels and three variables as shown in Table 3 and Table 4. Each run was done independently while glauconite and kaolin dose varied according to the design.

Aliquots of Fe (II) solutions of known concentration were put into the glass bottles (100 ml) containing accurately weighted amounts of the adsorbent. After the required adsorption time, iron ions concentration was determined by atomic absorption flame emission spectrophotometer (AA-6200 Shimadzu).

2.3. Cation Exchange Capacity (CEC)

25.0 g of clay sample was added to a 500 ml Erlenmeyer flask, then, 125 ml of 1 M NH_4OAc added with shaking thoroughly and allows standing 16 hours. After standing, filtrate the sample then, wash and rinse with eight separate addition of 95% ethanol to remove excess saturating solution. Extract the adsorbed NH_4 by leaching the sample with eight separate 25 ml additions of 1 M KCl. Discard the clay sample and transfer the lechate to a 250ml volumetric flask. Dilute to volume with additional KCl. The concentration of NH_4-N in the KCl extract was determined by spectrophotometer (spectro UV-2650, LABOMED, USA) [29].

Table 1. XRF analysis for natural glauconite and kaolin

Elements	Glauconite	Kaolin
SiO_2 (%)	39.0	51.6
Al_2O_3 (%)	23.50	29.7
K_2O (%)	3.50	0.48
Fe_2O_3 (%)	23.88	2.48
CaO (%)	0.04	0.27
TiO_2 (%)	----	0.14
P_2O_5 (%)	0.37	0.54
MnO (%)	0.05	0.75
Cl (%)	0.20	----
SO_3 (%)	1.52	0.09
L.O.I (%)	7.05	13.54

Table 2. Physical properties of glauconite and kaolin

Parameters	Value	
	Glauconite	Kaolin
Specific surface area (m^2/g)	19.8	5.4
CEC (meq/100 g)	28	11
Porous volume (cm^3/g)	0.264	0.315
Particle size (µm)	80-100	80-100

Table 3. Experimental Box-Behnken design with three levels and three variables applied in adsorption experiments

Run no.	Codec factor levels		
	Time	Concentration	Dose
1	-1	+1	0
2	0	-1	-1
3	+1	0	+1
4	+1	-1	0
5	-1	0	-1
6	-1	-1	0
7	0	0	0
8	0	-1	+1
9	0	0	0
10	0	+1	+1
11	0	0	0
12	0	0	0
13	0	0	0
14	-1	0	+1
15	0	+1	-1
16	+1	0	-1
17	+1	+1	0

2.4. Morphology Analysis

In order to know the reason of highly effective removal of iron with glauconite, structure sight should be analyzed. Scanning electron microscope (SEM) (JEOL instrument, Japan, model JSM-5410) was employed to visualize sample morphology. In the present work, the glauconite sample was analyzed by this technique using SEM to study the surface morphology of glauconite sample.

2.5. Statistical analysis

Box-Behnken design was used for statistical experimental design [30] to study, know the interactions and analyze the effects of studied parameters on the iron ions adsorption efficiency at glauconite and kaolin.

Table 4. Codec factor variables

Variables	Levels		
	0	+1	-1
Time (min)	35	60	10
Concentration (mg/L)	20	30	10
Dose (g)	0.55	1.0	0.1

According to this design, the optimal conditions were estimated using a second order polynomial function by which correlations between studied parameters (time, concentration & dose) and response (adsorption efficiency, %) were established. The general form of this equation is given in Eq. 1, Where Y is the predicted response, X_1, X_2 and X3 are the studied variables;β_i are equation constants and coefficients. Software package, Design-Expert 9.0.3, Stat-Ease, Inc., MN, USA, was used for regression analysis of experimental data and to plot response surface contours.

$$Y = \beta_o + \beta_1X_1 + \beta_2X_2 + \beta_3X_3 + \beta_{12}X_1X_2 + \beta_{13}X_1X_3 + \beta_{23}X_2X_3 + \beta_{11}X_1^2 + \beta_{22}X_2^2 + \beta_{33}X_3^2 \quad (1)$$

3. Results and Discussion

3.1. Characterization of Glauconite and Kaolin

Some chemical and physical properties of glauconite and kaolin are presented in Table 1 and Table 2. The glauconite sample has a specific surface area 19.8m^2/g while kaolin 5.4m^2/g. Also, CEC of glauconite was 28 meq/100 g and kaolin was 11meq/100 g.

3.2. Statistical analysis of variance Fe(II) adsorption

Adsorption results of iron ions on glauconite and kaolin are given in Table 5. The adsorption efficiency (%) onto glauconite was varied from 14.8 to 95.3% (Run numbers 5 and 8). More than 95% Fe (II) removal with contact time 35 minutes, iron load 10 mg/L and 1.0 g of glauconite. Actually, these results of glauconite are highly promised if it compared with Electro-coagulation method which give removal efficiency of Fe (II) 95-99 % with high coast (Approx. 6.05 \$/m^3) [31] while clay adsorption of glauconite and kaolin is not expensive because these ores has low price (24-39 \$ per ton of clay) [32]. In spite of the design conditions of iron ions adsorption efficiency (%) onto kaolin varied from 1.1 to 44 % (Run numbers. 16 and 8) where it's noticed the weak adsorption compared to glauconite, it still more economic in use than other techniques like electro-coagulation method and adsorption with activated carbon [31].

Statistical results of analysis of variance of Fe (II) adsorption on the surface of glauconite & kaolin are given in Table 6. The time of adsorption and adsorbent dose are the most significant factors while the concentration of adsorbate is less significant.

Table 5. Results of Fe (II) adsorption on the surface of glauconite & kaolin

Run no.	Time (min)	Concentration (mg/L)	Dose (g)	Adsorption (%)	
				Glauconite	Kaolin
1	10	30	0.55	48.7	2.4
2	35	10	0.10	64.6	19.6
3	60	20	1.00	95.2	23.7
4	60	10	0.55	94.0	20.4
5	10	20	0.10	14.8	9.4
6	10	10	0.55	62.0	32.7
7	35	20	0.55	84.5	10.5
8	35	10	1.00	95.3	44.0
9	35	20	0.55	84.5	10.3
10	35	30	1.00	73.0	3.6
11	35	20	0.55	84.5	10.6
12	35	20	0.55	84.8	10.5
13	35	20	0.55	84.5	10.4
14	10	20	1.00	45.3	14.7
15	35	30	0.10	28.6	1.1
16	60	20	0.10	45.8	8.2
17	60	30	0.55	92.2	2.9

The obtained correlation coefficient (R^2) of the models was 0.94, which indicates a good predictability of the models. It is noticed that, for kaolin, the concentration of adsorption is the most significant while the time of adsorption and adsorption dose are less significant. The obtained correlation coefficient (R^2) of the models was 0.92, which indicates a good predictability of the models.

The correlation between adsorption efficiency (%) and process factors (time, concentration and dose) can be shown as indicated in equations (2) and (3) in terms of the actual factors for glauconite and kaolin, respectively:

$$\text{Adsorption} = +84.22 + 19.56 * A - 9.18 * B + 19.38 * C + 2.88 * AB + 4.74 * AC + 3.42 * BC - 12.75 * A^2 + 12.57 * B^2 - 21.42\, C^2 \quad (2)$$

$$\text{Adsorption} = +33.85 - 0.4 * A - 1.11 * B + 29.65 * C + 0.01 * AB + 0.23 * AC - 1.22\, BC \quad (3)$$

where A is the time of adsorption (min), B is the concentration of ferrous ions (mg/L) and C is the glauconite or kaolin dose (g per 100 ml solution).

These equations are highly significance because they represent the net results of statistical application input data, so by known any adsorption parameters of time, concentration and glauconite or kaolin dose, by applied directly in equation (2) or (3), output results will be adsorption efficiency (%).

Table 6. Analysis of variance of Fe (II) adsorption on the surface of glauconite & kaolin

Source	Sum of Squares		Mean Square		F-Value		p-value (Prob > F)	
	Glauconite	Kaolin	Glauconite	Kaolin	Glauconite	Kaolin	Glauconite	Kaolin
Model	9632.7	1896.4	1070.3	316.1	31.1	18.7	< 0.0001	<0.0001
A (Time)	3059.6	2.0	3059.6	2.0	89.1	0.1	< 0.0001	0.7383
B (Concentration)	673.5	1423.1	673.5	1423.1	19.6	83.9	0.0031	<0.0001
C (Dose)	3005.1	284.4	3005.1	284.4	87.4	16.8	< 0.0001	0.0022
AB	33.1	40.9	33.1	40.9	0.9	2.4	0.3594	0.1511
AC	89.8	26.0	89.8	26.1	2.6	1.5	0.1501	0.2437
BC	46.9	119.9	46.9	119.9	1.4	7.1	0.2809	0.0239
A^2	664.9	---	664.9	---	19.3	---	0.0032	---
B^2	27.8	---	27.8	---	0.8	---	0.3981	---
C^2	1931.2	---	1931.2	---	56.2	---	0.0001	---

3.2. Interaction of the studied parameters

3.2.1. Effects of adsorption time and Fe (II) ions concentrations on adsorption efficiency

Effects of adsorption time and Fe (II) ions concentrations on adsorption efficiency at doses (0.55 g per 100 ml solution) for glauconite and kaolin are given in Figure 1. The adsorption efficiency of Fe (II) onto glauconite and kaolin increased by increasing adsorption time at all the glauconite and kaolin doses studied.

With addition 0.55 g of glauconite dose, the adsorption efficiency increased from 60-70 % to 100 % with increasing adsorption time from 10 to 60 minutes at low Fe (II) concentration of 10 mg/L (Figure 1A). At high Fe (II) concentration of 30 mg/L and also with 0.55 g of glauconite dose, the adsorption efficiency increased from 40-50 % to 80-90 % with increasing adsorption time from 10 to 60 minutes (Figure 1A). While, with the addition of 0.55g of kaolin, the adsorption efficiency increases up to 30 % with increasing adsorption time from 10 to 60 minutes and decreases Fe (II) concentration from 30 to 10 mg/L (Figure 1B).

3.2.2. Effects of adsorption time and glauconite dose on adsorption efficiency

Effects of adsorption time and dose of glauconite and kaolin on adsorption efficiency at Fe (II) ions concentration (10 mg/L) are given in Figure 2. The adsorption efficiency of Fe (II) onto glauconite increases by increasing adsorption time. The results reveal that with 0.1 g of glauconite dose, the adsorption efficiency increases from 40-50 % to 60-70 % with increasing adsorption time from 10 to 60 minutes at low Fe (II) concentration of 10 mg/L (Figure 2A).

However, at high glauconite dose of 1.0 g and at low Fe (II) concentration of 10 mg/L, the adsorption efficiency increases from 60-70 % to about 100 % with increasing adsorption time from 10 to 60 minutes (Figure 2A).

While, the effect of interaction of two factors; the time of adsorption and kaolin dose on adsorption efficiency at Fe (II) ions concentration (10 mg/L) was shown in Figure 2B. It can be observed that beyond the adsorption time of 10 minutes, the adsorption efficiency increases slowly from 10 to 35% with increasing time of adsorption from 10 to 60 minutes and the dose of kaolin increasing from 0.1 to 1.0 g (Figure 2B).

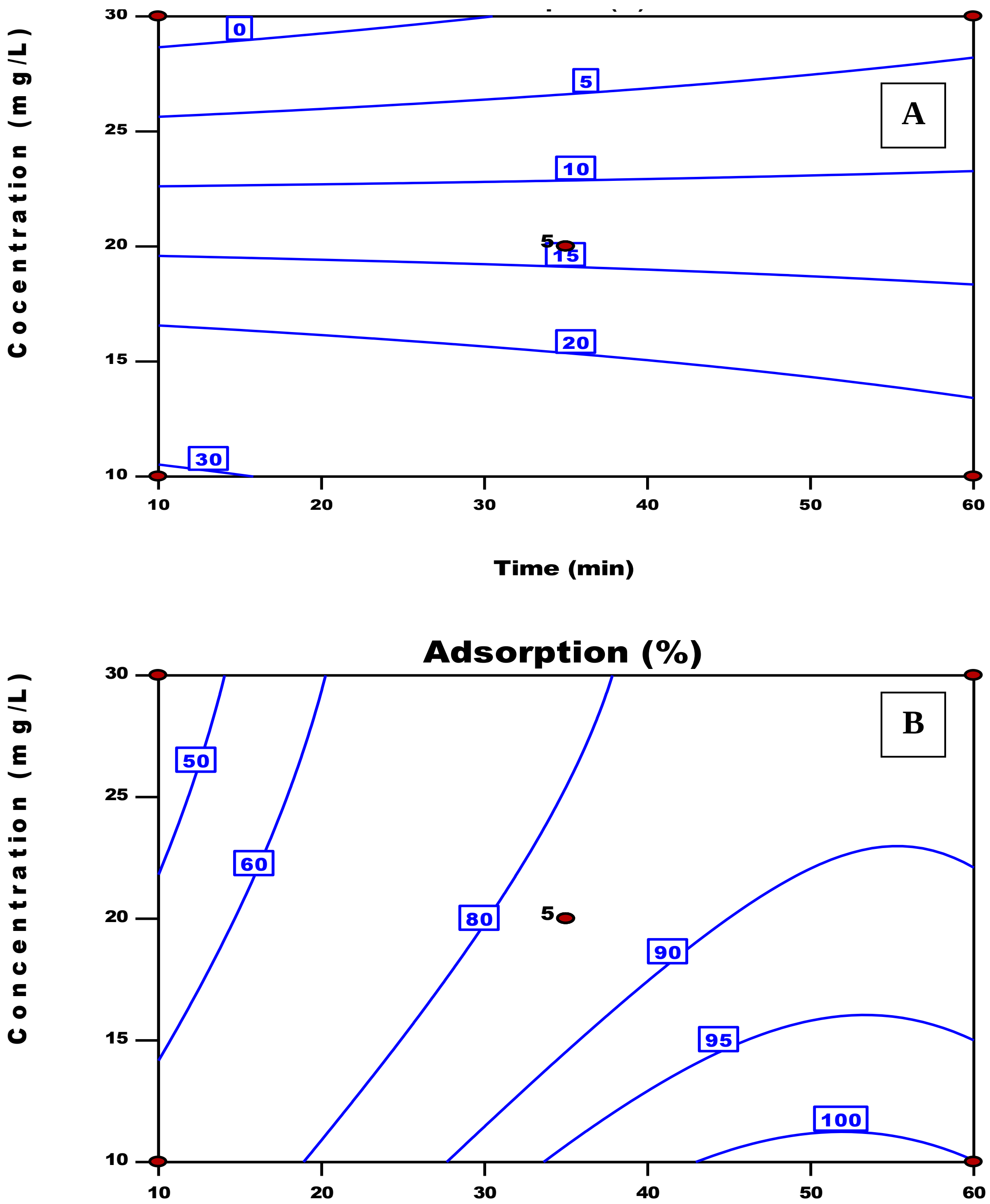

Figure 1. Effect of adsorption time and Fe (II) concentration on adsorption efficiency at dose = 0.55 g of glauconite "A" & kaolin "B"

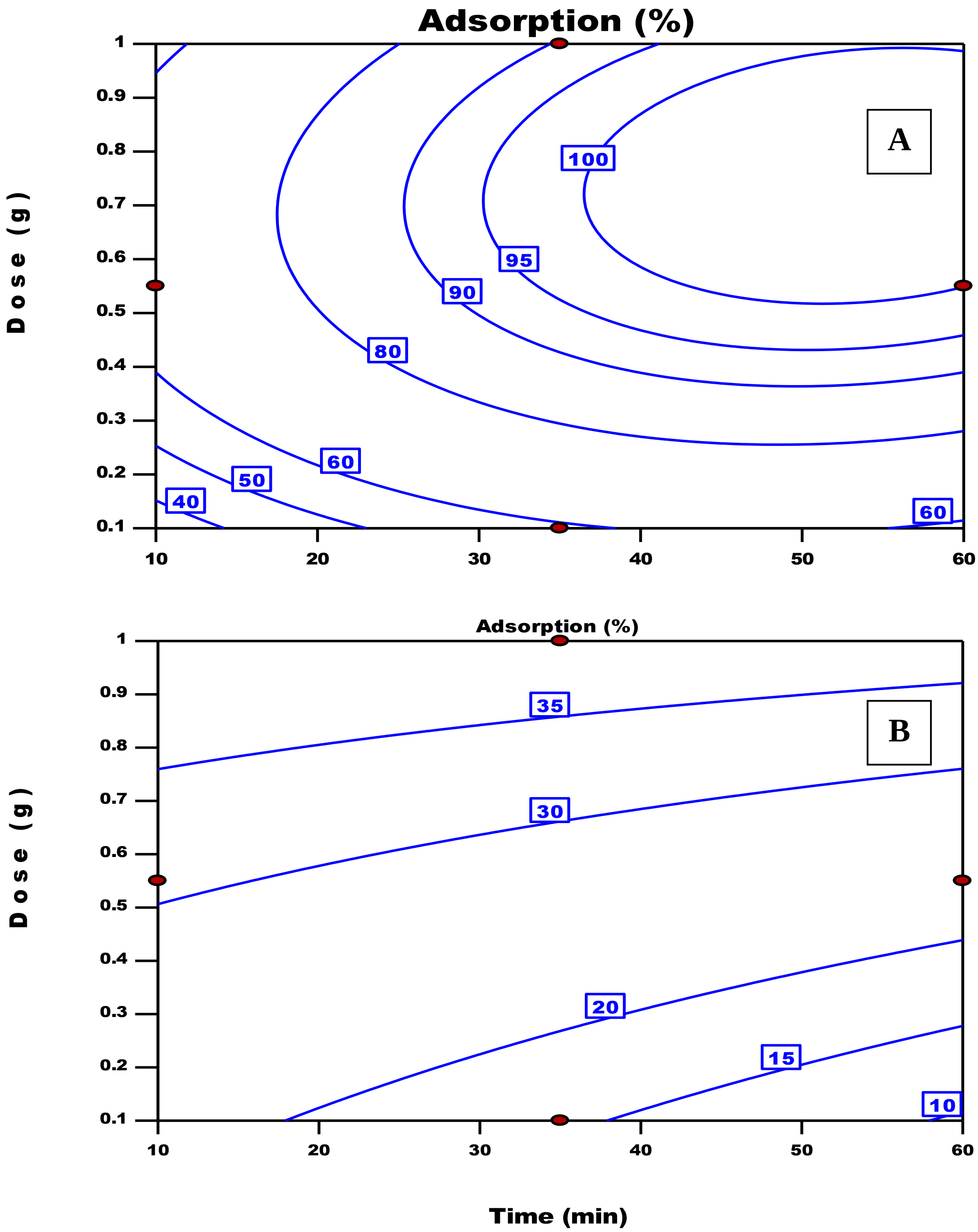

Figure 2. Effect of adsorption time and glauconite "A" & Kaolin "B" dose on adsorption efficiency at 10 mg/L concentration of Fe (II)

3.2.3. Effects of Fe (II) ions concentrations and kaolin doses on adsorption

Effects of Fe (II) ions concentrations and doses of glauconite and kaolin on adsorption efficiency at adsorption time (60 minutes) are given in Figure 3. These results reveal that, the adsorption efficiency of Fe (II) onto glauconite slightly decreased with increasing ferrous ions concentrations. On the other hand, the adsorption efficiency of Fe (II) onto glauconite increased by increasing glauconite dose.

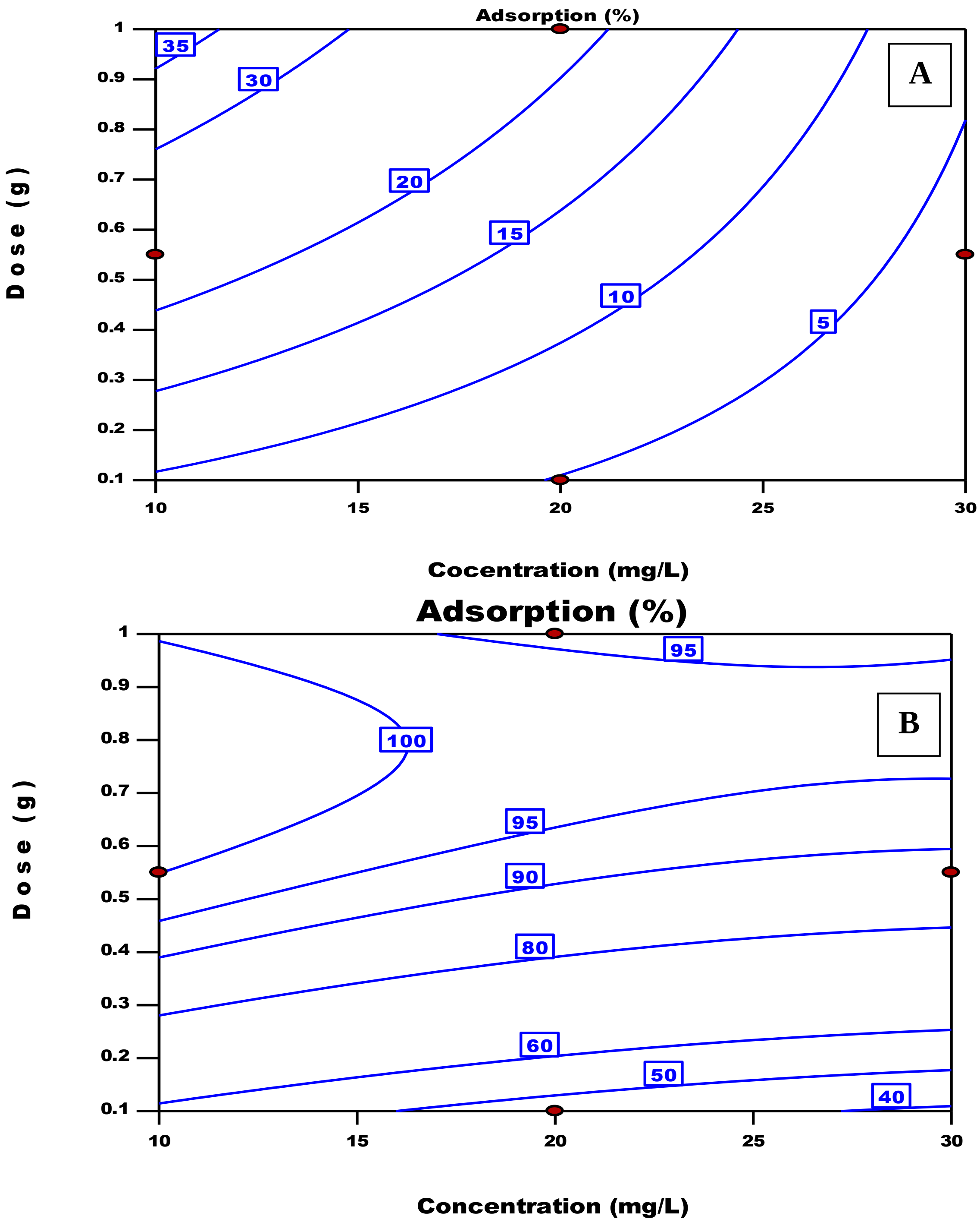

Figure 3. Effect of Fe(II) concentration and glauconite "A" & kaolin "B" dose on adsorption efficiency at 60 min. times adsorption

Moreover, at high adsorption time of 60 minutes with 0.1 g of glauconite dose, the adsorption efficiency decreased from 50-60 % to about 40 % with increasing ferrous ions concentrations from 10 to 30 mg/L (Figure 3A). However, at high glauconite dose of 1.0 g and at the same adsorption time of 60 minutes, the adsorption efficiency decreased from about 100 % to 95-100 % with increasing ferrous ions concentration from 10 to 30 mg/L (Figure 3A).

However, the adsorption efficiency of kaolin decreased from 35% to 5% with increase concentration of Fe (II) ions (Figure 3B).

All the experimental results of glauconite have been plotted at the 3-D cube graph as shown in Figure 4. From this cube, the highest adsorption efficiency 99.4 % was obtained at high dose of glauconite, low concentration of Fe (II) and high adsorption time. The lowest removal efficiency of about 3.1 % was obtained at the lowest dose of glauconite, the lowest time interval and at the highest concentration of Fe (II).

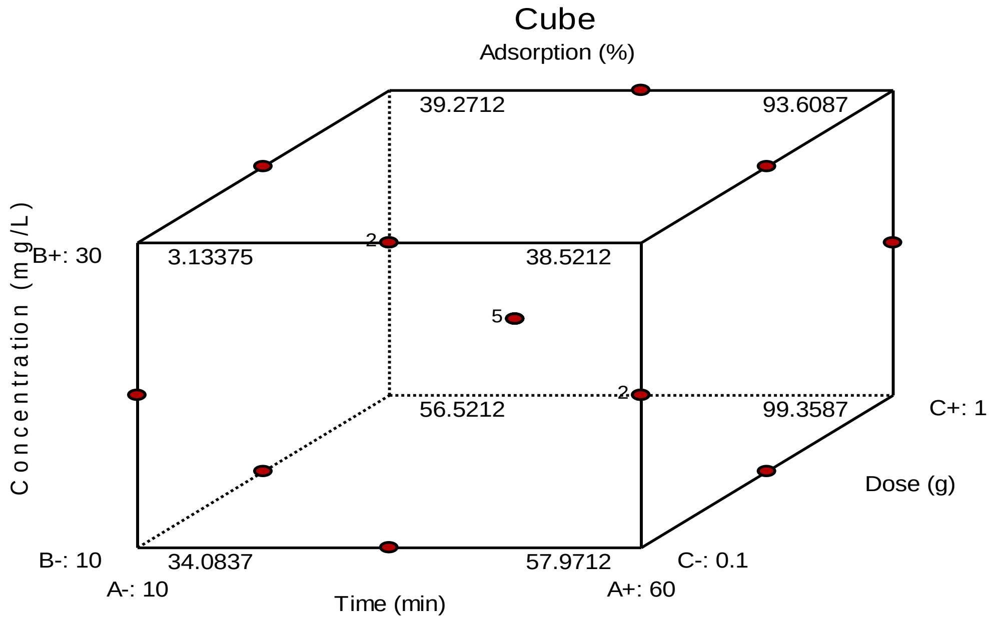

Figure 4. 3-D plot for the results of Fe (II) adsorption on glauconite

All experimental data of kaolin have been collected at the 3-D cube as shown in Figure 5. This cube shows that the highest adsorption efficiency 39.7 % can be obtained at high dose of kaolin, low concentration of ferrous ions and with no significance for adsorption time. At the lowest dose of glauconite, the lowest time interval and at the highest concentration of ferrous ions the results show high desorption on the surface of kaolin.

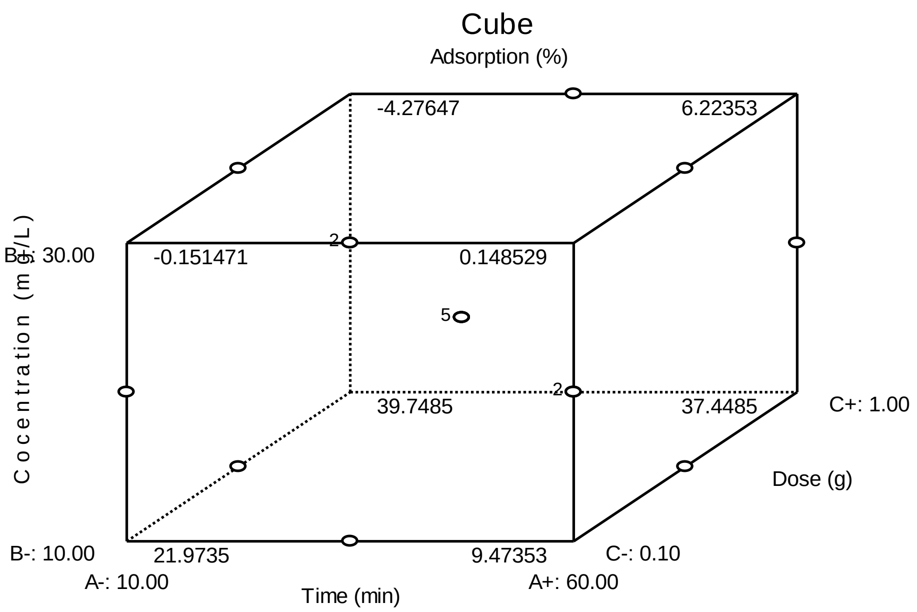

Figure 5. 3-D plot for the results of Fe (II) adsorption on kaolin

3.3. Surface morphology

SEM images with different levels of magnification factor are taken for glauconite sample in order to show the major features of the structure sight of glauconite surface. Figures 6A & 6B show the SEM images for glauconite sample with magnification factor 10,000 and 25,000, respectively. It is obvious that the high surface roughness increase the surface area of adsorption.

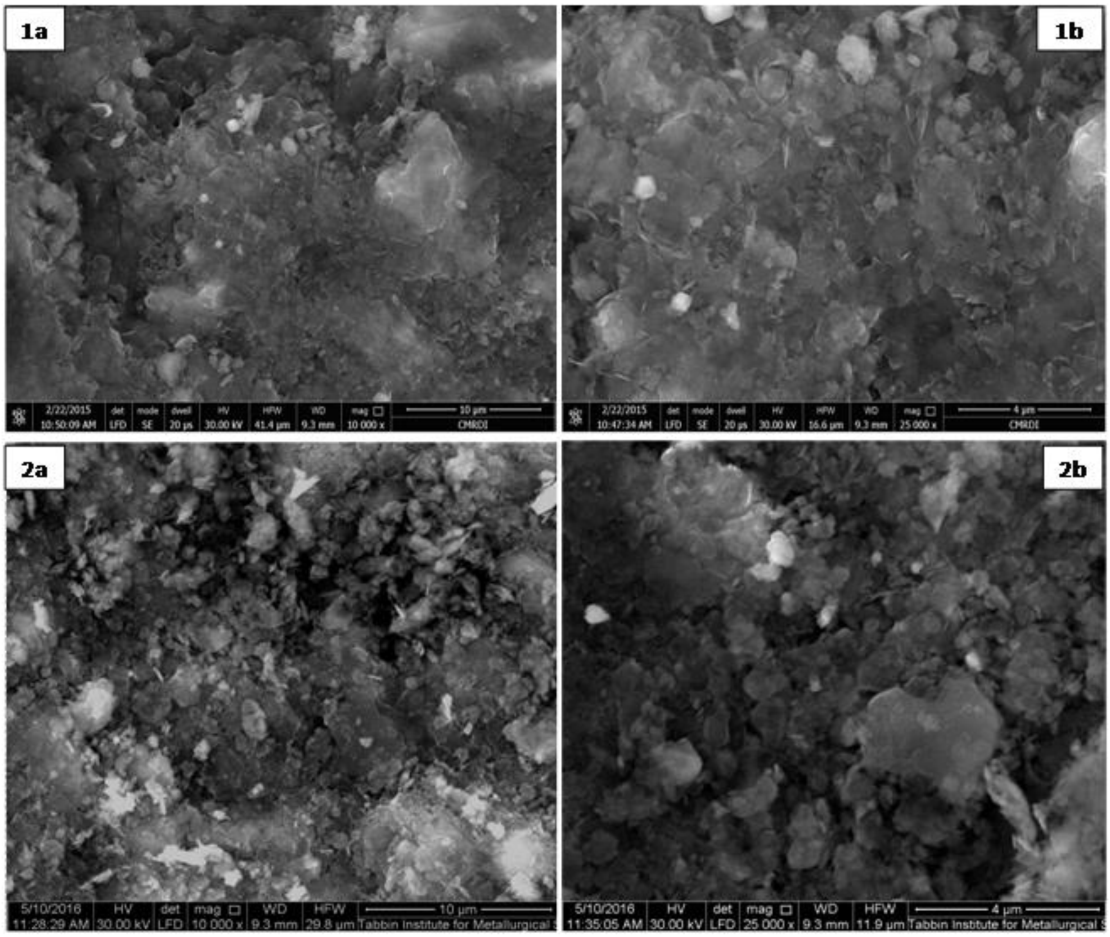

Figure 6. Representative SEM images of glauconite with magnification factor (1a. x10 000 and 1b. x25 000) and kaolin with magnification factor (2a. 10 000x and 2b. x 25 000)

4. Conclusion

Adsorption of ferrous ions on glauconite and kaolin were studied. Statistical experimental design of 3 variables and 3 levels is applied. The interactions of all the adsorption parameters (adsorption time, ferrous ions concentration and adsorbate dose) and their effects on adsorption efficiency are discussed. All the experimental results have been plotted at the 3-D cube graph. For glaucconite, the results reveal that, the highest adsorption efficiency of 99.4% is achieved at high dose of glauconite, low concentration of Fe (II) and high adsorption time. The lowest removal efficiency of about 3.1 % can be obtained at the lowest dose of glauconite, the lowest adsorption time and at the highest concentration of Fe(II). For kaolin, the results reveal that, the highest adsorption efficiency of 39.7 % is achieved at high dose of kaolin, low concentration of ferrous ions and with no significance for adsorption time.

From economic point of view, using the lowest glauconite dose and the highest adsorption time with low ferrous ions concentrations gives 50% to 60% adsorption efficiency. So, multi-stage adsorption will be cost-effective. While for kaolin, it give low adsorption efficiency and there is no high significance effect for iron removal with compared to glauconite.

References

1. D. Mohan, C.U. Pittman Jr., Review Activated Carbons and Low Cost Adsorbents for Remediation of Triand Hexavalent Chromium from Water, J Hazard Mater. 2006;137:762-811.
2. Y.C. Sharma, V. Srivastava, V.K. Singh, S.N. Kaul, C.H. Weng, Nano-Adsorbents for Removal of Metallic Pollutants from Water and Wastewater, Environ Technol. 2009;30:583-609.
3. K. Bhattacharyya, S.S. Gupta, Adsorption of Chromium (VI) from Water by Clays, Ind Eng Chem Res. 2006; 45: 7232-40.
4. G. Yuan, L. Wu, Allophane nanoclay for the removal of phosphorus in water and wastewater, Sci Technol Adv Mat. 2007;8:60-2.
5. P. Monvisade, P. Siriphannon, Chitosan intercalated montmorillonite: Preparation, characterization and cationic dye adsorption, Appl Clay Sci. 2009; 42: 427-31.
6. M. M. Nasef, A. H. Yahya, Adsorption of some heavy metal ions from aqueous solutions on Nafion 117 membrane, Desalination 2009; 249: 677-81.
7. M. Zaw, B. Chiswell, Iron and manganese dynamics in lake water, Water Res. 1999; 33: 1900-10.
8. A. Wolthoom, E.J.M. Temminghoff, L. Weng, W.H. Van Riemsdijk, Colloid formation in groundwater: effect of phosphate, manganese, silicate and dissolved organic matter on the dynamic heterogeneous oxidation of ferrous iron, Appl Geochem. 2004; 19: 611–22.
9. O. Yavuz, Y. Altunkaynak, F. Guzel, Removal of copper, nickel, cobalt and manganese from aqueous solution by kaolinite, Water Res. 2003; 37: 48-952.
10. A. Acra, R. Milki, Y. Karahagopian, Changes in quality of thermal groundwater from unique resources in Lebanon, Int. J. Environ. Studies; 1981; 19: 63-8.
11. Gu. Xueyuan, Les j. Evans, Barabash, J. Sara, Modeling the adsorption of Cd(II), Cu(II), Ni(II), Pb(II) and Zn(II) onto montmorillonite, Geochim Cosmochim Acta. 2010; 74: 5718-28.
12. M.E. Ossman, M. Abdel-Fatah, Nahla A. Taha, Fe(III) removal by activated carbon produced from Egyptian rice straw by chemical activation, Desaliantion Water Treatment Journal; 2014; 52: 3159 - 68.
13. O. Abollino, M. Aceto, M. Malandrino, Adsorption of heavy metals on Na-montmorillonite: Effect of pH and organic substances, Water Res. 2003; 37: 1619-27.
14. Y.H. Li, J. Ding, Z. Luan, Competitive adsorption of Pb^{2+}, Cu^{2+} and Cd^{2+} ions from aqueous solutions by multiwalled carbon nanotubes, Carbon; 2003; 41: 2787-92.
15. Y.H. Li, S. Wang, J. Wei, Lead adsorption on carbon nanotubes, Chem Phys Lett. 2002; 357; 263-6.
16. Z. Gao, T.J. Bandosz, Z. Zhao, Investigation of factors affecting adsorption of transition metals on oxidized carbon nanotubes, J Hazard Matter. 2009; 167: 357-65.
17. X. Guo, S. Zhang, X. Q. Shan, Adsorption of metal ions on lignin, J Hazard Matter. 2008; 151: 134-42.
18. S. Debnath, U. C. Ghosh, Nanostructured hydrous titanium (IV) oxide: Synthesis, characterization and Ni (II) adsorption behavior, Chem Eng J. 2009; 152: 480-91.
19. S.E. O'Reilly, M.F. Hochella, Lead sorption efficiencies of natural and synthetic Mn and Fe-oxides, Geochim. Cosmochim; 2003; 67: 4471-87.
20. R.O. James, T.W. Healy, Adsorption of hydrolyzable metal ions at the oxide-water interface. I. Co(II) adsorption on SiO_2 and TiO_2 as model systems, J Colloid Interface Sci. 1972; 40: 42-52.

21. K.M. Spark, B.B. Johnson, J.D. Wells, Characterizing heavy-metal adsorption on oxides and oxyhydroxides, Eur J Soil Sci. 1995; 46: 621-31.

22. E.A. Forbes, A.M. Posner, J.P. Quirk, The Specific Adsorption of Divalent Cd, Co, Cu, Pb, and Zn on Goethite, J Soil Sci. 1976;27:54-166.

23. M.M. Benjamin, J.O. Leckie, Competitive adsorption of Cd, Cu, Zn, and Pb on amorphous iron oxyhydroxide, J. Colloid Interface Sci. 1981;83:410-19.

24. B. Nowack, L. Sigg, Adsorption of EDTA and Metal-EDTA Complexes onto Goethite, J. Colloid Interface Sci. 1996; 177: 106-21.

25. C.C. Ainsworth, J.L. Pilon, P.L. Gassman, W.G. Van Der Sluys, Cobalt, Cadmium, and Lead Sorption to Hydrous Iron Oxide: Residence Time Effect, Soil Sci Soc Am J. 1994; 58: 1615-23.

26. P.H. Tewari, A.B. Campbell, W. Lee, Adsorpption of Co^{2+} by Oxides from Aqueous solution, Can J Chem. 1972; 50: 1642-8.

27. B.B. Johnson, Effect of pH, temperature, and concentration on the adsorption of cadmium on goethite, Environ Sci Technol. 1990; 24: 112-8.

28. L.G.J. Fokkink, A. de Keizer, J. Lyklema, Temperature dependence of cadmium adsorption on oxides: I. Experimental observations and model analysis, J. Colloid Interface Sci. 1990; 135: 118-31.

29. H.D. Chapman, Cation-exchange capacity. *In:* C.A. Black (ed.). Methods of soil analysis - Chemical and microbiological properties. Agronomy. 1965; 9: 891-901.

30. G.E.P. Box, D.W. Behnken, Technometrics; 1960; 2: 455.

31. S. Chaturvedi, P. N. Dave, Removal of iron for safe drinking water, Desalination. 2009; 303: 1-11.

32. Ö. Yavuz, R. Guzel, F. Aydin, I. Tegin, R. Ziyadanogullari, Removal of Cadmium and Lead from Aqueous Solution by Calcite, Polish J Environ Stud. 2007; 16(3): 467-71.